

# A shock solution for the nonlinear shallow water equations

MATTEO ANTUONO†

US3, INSEAN, via di Vallerano 139, Rome 00128, Italy

(Received 6 November 2009; revised 26 March 2010; accepted 26 March 2010;  
first published online 17 June 2010)

A global shock solution for the nonlinear shallow water equations (NSWEs) is found by assigning proper seaward boundary data that preserve a constant incoming Riemann invariant during the shock wave evolution. The correct shock relations, entropy conditions and asymptotic behaviour near the shoreline are provided along with an in-depth analysis of the main quantities along and behind the bore. The theoretical analysis is then applied to the specific case in which the water at the front of the shock wave is still. A comparison with the Shen & Meyer (*J. Fluid Mech.*, vol. 16, 1963, p. 113) solution reveals that such a solution can be regarded as a specific case of the more general solution proposed here. The results obtained can be regarded as a useful benchmark for numerical solvers based on the NSWEs.

**Key words:** surface gravity waves, wave breaking

---

## 1. Introduction

Breaking waves on beaches have always been a fundamental research topic in the analysis of the nearshore zone dynamics and related phenomena. This is mainly due to the fact that breaking waves act as a forcing for rip and longshore currents (Guard & Baldock 2007; Brocchini & Dodd 2008; Zhang & Liu 2008) and further represent one of the main causes of sediment transport and erosion on sandy beaches (Elfrink & Balbock 2002; Pritchard & Hogg 2005). Hence, accurate and correct modelling of wave breaking phenomena and breaking wave motion is a crucial issue for all scientists who are interested in coastal phenomena (e.g. Synolakis 1987; Antuono & Brocchini 2008; Chang, Hwang & Hwung 2009).

With respect to this, analytical solutions are of fundamental importance for the assessment of the accuracy of any numerical solver used to model the nearshore dynamics. In this context, the most widespread equations are the nonlinear shallow water equations (NSWEs), as they enable modelling of the wave breaking in a simple and reliable way. In fact, within the theory of hyperbolic systems, breaking is usually represented as a sharp discontinuity in the flow quantities (hence the name ‘shock wave’) which evolves satisfying specific conditions stemming from the laws of mass and momentum conservation (see, for example, Toro 1999, 2001; Wu & Cheung 2007).

Unfortunately, despite the great need for shock wave solutions, at present the analytical results available in the literature have a validity which is limited to short temporal and spatial domains. The first and most famous solution is that provided by Shen & Meyer (1963). Using an asymptotic analysis, they found the main features

† Email address for correspondence: [matteoantuono@gmail.com](mailto:matteoantuono@gmail.com)

of the bore evolution near the shoreline and during the run-up. Their solution is, however, local and holds only in a small neighbourhood of the point at which the bore collapses on the shore. The global behaviour (that is, for finite intervals of time and space) of the Shen & Meyer solution has been inspected by Peregrine & Williams (2001), who described the bore-induced run-up on a truncated beach. Further, a wider class of solutions for the run-up/run-down induced by a bore has been recently found by Pritchard, Guard & Baldock (2008) through the definition of proper boundary conditions behind the shock wave. The main limitation of the latter two solutions is that they are based on the assignment of the boundary conditions on a moving curve which starts at the point of bore collapse. First, this implies that the region of validity of the solution is rather small and close to the shoreline. Further, the assignment along a moving curve makes the numerical implementation rather difficult. More recently Antuono, Hogg & Brocchini (2009) found an analytical solution for a similar problem but without the previous difficulties in the boundary data assignment. In any case, in all the cases cited above, the problem is not that of a natural bore climbing on a sloping beach but that of a dam break on a sloping plane. In fact, as shown by Whitham (1958) and Hibberd & Peregrine (1979), a natural bore has no discontinuity at the shoreline as a consequence of the so-called bore collapse at the shoreline and, therefore, cannot be modelled through a dam break problem.

In the present study, we provide a global solution for a special case of a shock wave. The boundary data are assigned along the seaward boundary of the sloping beach, that is, at  $x = -1$  ( $x$  being the dimensionless onshore coordinate) for all times, and the shock evolution is followed up to the run-up/run-down region. The paper is organized as follows: §1 introduces the NSWEs and their hyperbolic structure, §2 describes the shock relations and the entropy conditions while §3 is devoted to the definition of the boundary conditions. Finally, in §§4–6, the shock solution is illustrated along with the main results.

## 2. The NSWEs

For wavefronts approaching a uniformly sloping frictionless beach with a small incident angle (Ryrie 1983; Brocchini & Peregrine 1996), the onshore problem of weakly two-dimensional NSWEs (in dimensionless form) is

$$\left. \begin{aligned} d_t + Q_x &= 0, \\ Q_t + \left[ \frac{d^2}{2} + \frac{Q^2}{d} \right]_x &= h_x d, \end{aligned} \right\} \quad (2.1)$$

where  $Q = u d$  is the onshore flux,  $u$  is the onshore velocity,  $d = h + \eta$  is the total water depth,  $\eta$  is the free surface elevation,  $h = -x$  is the still-water depth and subscripts represent partial differentiation. The axes' origin is posed at the undisturbed shoreline; the  $x$ -coordinate gives the onshore direction and points in the landward direction ( $x, z$ ) forming a right-handed Cartesian reference frame (see figure 1). The scale factors for vertical lengths, horizontal lengths and times are, respectively, the still-water depth at the seaward boundary  $h_0^* = h^*(x = -1)$ ,  $h_0^* / \tan \theta$  and  $t_0^* = \sqrt{h_0^* / g} / \tan \theta$ , where  $\tan \theta$  is the beach slope,  $\theta$  the angle of the plane beach with respect to the horizontal plane and the starred variables indicate dimensional variables. More details can be found in Brocchini & Peregrine (1996).

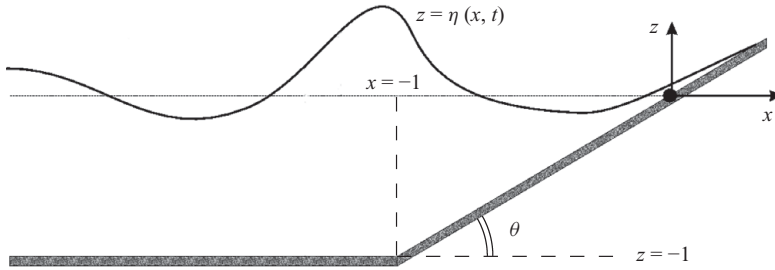


FIGURE 1. Sketch of geometry and flow dimensionless variables for the beach problem.

The system (2.1) is hyperbolic and can be cast into its characteristic form by using the following characteristic variables:

$$\alpha = u + t + 2c, \quad \beta = u + t - 2c, \tag{2.2}$$

where  $c = \sqrt{d}$ . Using  $\alpha$  and  $\beta$ , the system (2.1) becomes

$$\left. \begin{aligned} d\alpha/dt = 0, \quad \text{on curves such that } dx/dt = u + c, \\ d\beta/dt = 0, \quad \text{on curves such that } dx/dt = u - c. \end{aligned} \right\} \tag{2.3}$$

The curves defined in (2.3) are called characteristic curves. When the flow is subcritical (that is,  $u - c < 0 < u + c$ ), we call the former ones ‘incoming’, since they move from the seaward boundary ( $x = -1$ ) to the shoreline and the latter ones ‘outgoing’, since they move towards the opposite direction. As pointed out in Antuono & Brocchini (2007), the former curves carry information on the incoming waves entering the seaward boundary while the latter ones carry information on the wave reflection at the shoreline.

### 3. Shock relations

In this section we summarize the shock relations for the NSWs in order to give a simpler treatment of the shock wave evolution and asymptotic behaviour.

Before proceeding to the analysis, we underline that the term ‘shock wave’ is borrowed from the gas dynamics literature, while in the hydraulic context it is common to refer to a ‘hydraulic jump’ for the stationary discontinuity and to a ‘bore’ for the moving discontinuity. In any case, in the present study we adopt the nomenclature used in the theory of hyperbolic systems and, therefore, we refer to a shock wave to indicate a sharp discontinuity in the solution of the NSWs.

The dimensionless shock relations for the NSWs are

$$s [d] = [Q], \tag{3.1a}$$

$$s [Q] = \left[ \left[ \frac{d^2}{2} + \frac{Q^2}{d} \right] \right], \tag{3.1b}$$

where  $s$  is the shock wave velocity and  $[f] = f_2 - f_1$  represents the jump of the quantity  $f$  across the discontinuity. The subscript ‘2’ indicates the values seaward of the shock wave while ‘1’ indicates the values shoreward of the shock wave.

Substituting (3.1a) into (3.1b), we obtain the following:

$$s^2 (d_2 - d_1) = \frac{1}{2} (d_2 + d_1) (d_2 - d_1) + \frac{Q_2^2}{d_2} - \frac{Q_1^2}{d_1}. \tag{3.2}$$

Now we have two possible choices. In the first case we extract  $Q_2$  from (3.1a), substitute it into (3.2) and finally solve for  $s$ , obtaining

$$s = u_1 \pm \sqrt{\frac{1}{2} \left( \frac{d_2^2}{d_1} + d_2 \right)}. \quad (3.3)$$

In the second case we extract  $Q_1$  from (3.1a), substitute it into (3.2) and again solve for  $s$ , obtaining

$$s = u_2 \pm \sqrt{\frac{1}{2} \left( \frac{d_1^2}{d_2} + d_1 \right)}. \quad (3.4)$$

It is evident that (3.3) and (3.4) (as well as (3.1a) and (3.1b)) are linked by the symmetry  $(d_2, u_2) \leftrightarrow (d_1, u_1)$ . As a consequence, a choice of the signs in front of the square roots is not possible unless proper breaking-symmetry conditions are introduced.

### 3.1. Entropy conditions

The proper way to break the symmetry is to use the so-called entropy conditions. Such conditions have been built to avoid non-physical solutions of hyperbolic systems and to enable recovery of the uniqueness of the solution.

The term ‘entropy condition’ is borrowed from gas dynamics, and refers to the fact that the variation of entropy in a gas must satisfy the second law of thermodynamics. In the NSWs there is no entropy equation and the second law of thermodynamics is replaced by the request that the time variation of the water energy across the shock wave is non-positive. Following Stoker (1957) and adapting his results to the notation at hand, we obtain

$$\frac{dE}{dt} = \frac{m}{2d_1d_2} [d]^3 \leq 0, \quad (3.5)$$

where  $E$  is the water energy and  $m = (u_2 - s)d_2 = (u_1 - s)d_1$  is the mass flux across the shock wave (note that this quantity is continuous). The inequality (3.5) is satisfied when  $m \leq 0$ ,  $[d] \geq 0$  or  $m \geq 0$ ,  $[d] \leq 0$ . As we prove in the following, these conditions correspond to a shock wave generated, respectively, by the collapse of the  $\alpha$ - and  $\beta$ -characteristic curves.

The reasoning above requires the definition of the energy of the system and the related equation. Another approach is based on the use of the standard theory of hyperbolic systems. In this context, entropy conditions apply to each characteristic field of the hyperbolic system and fix a specific direction of propagation of the shock wave (see, for example, Toro 1999). Furthermore, since the shock wave must be ‘fed’ by the characteristic field associated with it, the shock velocity must be smaller than the velocity of the characteristic curves ‘behind’ the shock wave and greater than the velocity of the characteristic curves ‘in front’ of it. For shock waves generated by the collapse of the  $\alpha$ -characteristic curves, they are as follows,

$$u_2 + c_2 \geq s \geq u_1 + c_1, \quad (3.6)$$

while for shock waves generated by the collapse of the  $\beta$ -characteristic curves, they are as follows,

$$u_2 - c_2 \geq s \geq u_1 - c_1. \quad (3.7)$$

The ‘direction’ of the inequalities above is a consequence of the direction of the  $x$ -axis. As for the gas dynamics, conditions (3.6) and (3.7) imply that in the frame of

reference moving with the shock wave, the flow is supercritical ‘in front’ of the shock and subcritical ‘behind’ it.

In the following we let ‘ $\alpha$ -shock’ denote the shock wave generated by the collapse of the  $\alpha$ -characteristic curves and let ‘ $\beta$ -shock’ denote the shock wave generated by the collapse of the  $\beta$ -characteristic curves, even though we just deal with the  $\alpha$ -shock. Nevertheless, all the results found for the  $\alpha$ -shock can be adapted to the  $\beta$ -shock following the procedure shown in the following. Before proceeding to the analysis, we combine (3.3) and (3.4) as follows:

$$0 = u_2 - u_1 \pm \sqrt{\frac{1}{2} \left( \frac{d_1^2}{d_2} + d_1 \right)} \mp \sqrt{\frac{1}{2} \left( \frac{d_2^2}{d_1} + d_2 \right)}. \quad (3.8)$$

### 3.2. The $\alpha$ -shock

As a consequence of the entropy condition (3.6), relation (3.3) becomes

$$s = u_1 + \sqrt{\frac{1}{2} \left( \frac{d_2^2}{d_1} + d_2 \right)}. \quad (3.9)$$

Then, since (3.8) must be satisfied, relation (3.4) becomes

$$s = u_2 + \sqrt{\frac{1}{2} \left( \frac{d_1^2}{d_2} + d_1 \right)}, \quad (3.10)$$

and (3.8) can be rewritten as

$$u_2 - u_1 = (d_2 - d_1) \sqrt{\frac{1}{2} \left( \frac{1}{d_2} + \frac{1}{d_1} \right)}. \quad (3.11)$$

The expression (3.10) satisfies the entropy condition (3.6) if

$$\sqrt{d_2} \geq \sqrt{\frac{1}{2} \left( \frac{d_1^2}{d_2} + d_1 \right)}. \quad (3.12)$$

The former inequality is true if and only if  $d_2 \geq d_1$ . As a consequence of (3.11), it is  $u_2 \geq u_1$ . Finally, using (3.9), we get

$$d_2 = -\frac{d_1}{2} + \frac{1}{2} \sqrt{d_1^2 + 8d_1(s - u_1)^2}. \quad (3.13)$$

### 3.3. Asymptotic behaviour near the shoreline

As pointed out by Antuono & Brocchini (2007), the shoreline (that is, the line along which  $d=0$ ) is a singular curve for the NSWs. As a consequence, special behaviour of the shock waves is expected as  $d \rightarrow 0^+$ , that is, as the shoreline is approached.

Indeed, let us consider an  $\alpha$ -shock approaching the shoreline and assume that the shock velocity is always bounded. Then, using (3.9) and (3.10), the only way to get a finite value of  $s$  is that both  $d_1$  and  $d_2$  approach zero at the shoreline and that one of the following limits holds:

$$\frac{d_2^2}{d_1} = O(1) \quad \left( \text{or equivalently } \frac{d_1^2}{d_2} \rightarrow 0 \right), \quad \text{for } d_2, d_1 \rightarrow 0^+, \quad (3.14)$$

or

$$\frac{d_1^2}{d_2} = O(1) \quad \left( \text{or equivalently } \frac{d_2^2}{d_1} \rightarrow 0 \right), \quad \text{for } d_2, d_1 \rightarrow 0^+. \quad (3.15)$$

This is the so-called bore collapse and proves that  $[d]=0$  at the shoreline. In any case, since for the  $\alpha$ -shock  $d_2 \geq d_1$  ‘everywhere’, it follows that only (3.14) can be satisfied.

*Proof.* Let us assume that (3.15) is true for the  $\alpha$ -shock. Then, there exists a finite value  $m_1 > 0$  such that  $d_2 = m_1 d_1^2$  for  $d_2, d_1 \rightarrow 0^+$ . Since  $d_2 \geq d_1$ , it follows that

$$m_1 d_1^2 \geq d_1 \quad \text{for } d_1 \rightarrow 0^+ \quad \implies \quad d_1 \geq 1/m_1 > 0 \quad \text{for } d_1 \rightarrow 0^+,$$

which is not possible. Then, (3.15) is false and (3.14) is the correct choice.  $\square$

Finally, we note that (3.14) implies that  $d_2 = m_1 \sqrt{d_1}$  as  $d_1 \rightarrow 0^+$  ( $m_1$  is a positive value) and that using (3.10) yields  $s \rightarrow u_2$ . Substituting such relations into (3.9) and (3.10), we finally get

$$m_1 = \sqrt{2} (u_2 - u_1)|_{d_1=0}. \quad (3.16)$$

In the following we assume the variables in front of the shock wave (that is,  $d_1$  and  $u_1$ ) to be known.

#### 4. The boundary conditions: the $\alpha$ -constant $N$ -wave

Use of the relations found above to solve the shock wave evolution is a prohibitive task. Indeed, we have two known values, that is,  $d_1$  and  $u_1$ , and three unknowns, that is,  $d_2$ ,  $u_2$  and  $s$ . In principle, one could express the physical variables  $d_2$  and  $u_2$  as functions of the Riemann invariants  $\alpha_2$  and  $\beta_2$  behind the shock and then try to get  $\alpha_2$  by making the  $\alpha$  datum travel from the seaward boundary of the domain up to the shock rear side. In this case, the problem would be closed (i.e. we would have the same number of data and unknowns). In any case, the incoming characteristic curves are influenced by the field of the  $\beta$  invariant which, in turn, is influenced by the shock wave. As a consequence, the problem appears as a complex nonlinear interaction between the shock and the fields behind it.

To solve the problem we proceed as follows: we choose a boundary datum capable of generating an  $\alpha$ -constant field behind the shock wave. In this case, we know the value  $\alpha_2$  everywhere along the shock path and can close the equations given by the shock relations. As a consequence, before proceeding to the analysis, we dedicate the present section to the description of the boundary data.

As explained in Antuono & Brocchini (2007), when the flow is subcritical, the incoming characteristic curves are associated with the signals entering the sloping beach region, and the knowledge of such signals is necessary and sufficient to describe the global wave dynamics. Since the incoming curves carry the  $\alpha$  invariant, it follows that the only datum to be assigned at the seaward boundary (that is, at  $x = -1$ ) is  $\alpha$ . However, here we prefer to express the assignment problem through the physical variables  $u$  and  $c = \sqrt{d}$ . Specifically, we decompose them into an incoming component and a reflected component, that is, we set  $u(t, -1) = u^I(t) + u^R(t)$  and  $c(t, -1) = 1 + c^I(t) + c^R(t)$ . Since  $\alpha$  is associated only with the incoming components and  $\beta$  only with the reflected components, using (2.2) it follows that

$$\alpha = u^I + t + 2 + 2c^I \quad \implies \quad u^R = -2c^R, \quad (4.1)$$

$$\beta = u^R + t - 2 - 2c^R \quad \implies \quad u^I = 2c^I. \quad (4.2)$$

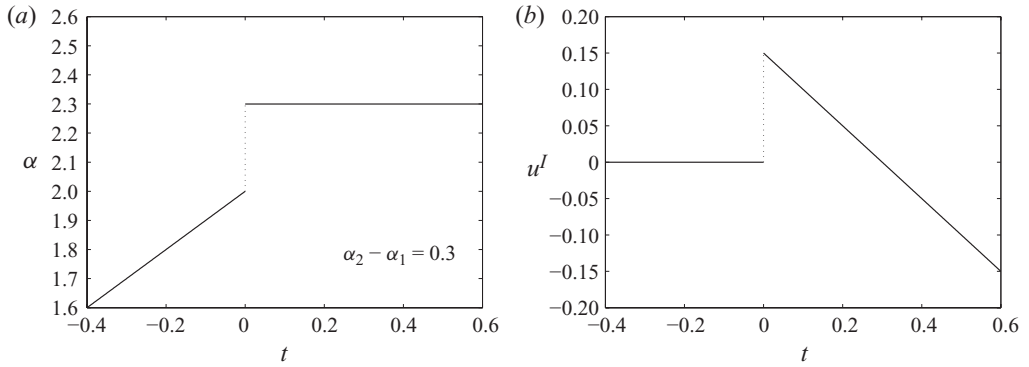


FIGURE 2. (a) The jump in the  $\alpha$ -field in the case of still water for  $t < 0$ . (b) The associated incoming signal  $u^I(t)$ .

Incidentally, we underline that such a decomposition is not possible when we use  $d$  and/or  $\eta$  since  $\alpha$  and  $\beta$  are not linearly dependent on such variables. Substituting the second relation of (4.2) into the first of (4.1), we finally get

$$\alpha = 2u^I + t + 2 = 4c^I + t + 2. \quad (4.3)$$

Now, let us assume the shock wave enters the domain at  $t = 0$  and  $\alpha \equiv \alpha_2$  for  $t > 0$ . Then, using (4.3), we obtain the boundary datum assignment

$$\alpha(t, -1) \equiv \alpha_2 = 2u^I(t) + t + 2 = 4c^I(t) + t + 2, \quad \forall t > 0, \quad (4.4)$$

and, therefore, we find

$$u^I(t) = \frac{\alpha_2 - 2 - t}{2}, \quad c^I(t) = \frac{\alpha_2 - 2 - t}{4}, \quad \forall t > 0. \quad (4.5)$$

The boundary data above are linearly decreasing functions of  $t$  and represent an N-wave (the wave shape resembles that of a letter ‘N’). Since such a wave induces a constant  $\alpha$ -field in the fluid region behind the shock wave, we call it the  $\alpha$ -constant N-wave. The problem is completely defined when the jump  $[\alpha] = \alpha_2 - \alpha_1$  at  $t = 0, x = -1$  is specified.

In figure 2(a) we illustrate one case in which the water is still for  $t < 0$  (that is,  $\alpha = 2 + t$ ) and  $\alpha \equiv \alpha_2 = 2.3$  for  $t > 0$ . In figure 2(b), the associated incoming signal  $u^I(t)$  is shown.

## 5. The shock solution

Let us consider the shock wave generated by the  $\alpha$ -constant N-wave defined in the previous section. Since  $\alpha_2$  is known along the shock path, the only unknowns are  $\beta_2$  and  $s$ . The dependence of the shock relations (3.9) and (3.10) on  $\beta_2$  is easily obtained by expressing  $u_2$  and  $d_2$  as functions of the Riemann invariants. Indeed, using (2.2), we get

$$u_2 = \frac{\alpha_2 + \beta_2}{2} - t, \quad d_2 = \frac{(\alpha_2 - \beta_2)^2}{16}. \quad (5.1)$$

At this stage, one would like to combine relations (3.9) and (3.10) in order to eliminate the dependence on  $\beta_2$  and make  $s$  explicit to solve the following initial value

problem:

$$\frac{dx}{dt} = s(d_1(x, t), u_1(x, t), t), \quad x(0) = -1. \quad (5.2)$$

Unfortunately, it is not possible to make  $s$  explicit, and we are forced to proceed as follows. First, we consider (3.11) and eliminate  $u_1$  and  $u_2$  using the definition of  $\alpha$ :

$$u_1 = \alpha_1 - 2\sqrt{d_1} - t = \alpha_1 - 2c_1 - t, \quad u_2 = \alpha_2 - 2\sqrt{d_2} - t = \alpha_2 - 2c_2 - t.$$

Then, after rearrangement, we get the following polynomial equation:

$$z^6 - 9c_1z^4 + 8\sqrt{c_1}(\alpha_2 - \alpha_1 + 2c_1)z^3 - [2(\alpha_2 - \alpha_1 + 2c_1)^2 + c_1^2]z^2 + c_1^3 = 0, \quad (5.3)$$

where  $z = c_2/\sqrt{c_1}$  (see Appendix A for more details). The polynomial in (5.3) admits six roots (both real and complex) and the correct root has to be chosen among the real ones through the entropy conditions. Specifically, since  $d_2 \geq d_1$ , the correct root is that satisfying  $z \geq \sqrt{c_1}$ . This root is evaluated numerically (as explained in detail in the following section) and used to get  $d_2$  and then  $s$  through (3.9). Finally, the shock velocity is used to integrate (5.2).

Note that, because of the entropy conditions, the variable  $z$  has order of magnitude equal to 1 all over the fluid domain (that is, offshore and nearshore). This ensures a uniform accuracy in the numerical evaluation of the roots.

## 6. Results

In the theoretical scheme described above, the fields  $d_1(x, t)$  and  $u_1(x, t)$ , which describe the flow dynamics in front of the shock wave, can be chosen in a general way. For the sake of simplicity, we assume that the water is still before the shock enters the sloping region and, therefore, we set  $u_1 \equiv 0$  and  $d_1 = \sqrt{-x}$  (see figure 2).

The polynomial roots of (5.3) have been computed using the Matlab built-in function `roots`, and the evaluation is stopped when  $d_1 \leq 10^{-12}$ . The numerical integration of (5.2) has been performed using a fourth-order Runge–Kutta scheme. The time step to be used as a reference inside the four substeps of the Runge–Kutta scheme is given by

$$dt = \tau_0 [1 - (1 - d_1)^n], \quad \text{with } n = 12, \tau_0 = 10^{-4}. \quad (6.1)$$

This choice is motivated by the request for a higher accuracy as the shock wave moves shoreward (that is, as  $d_1$  goes to zero). Indeed, the specific structure of (6.1) approximately gives  $dt \simeq \tau_0$  at the seaward boundary and in the middle part of the sloping region (where  $d_1 = O(1)$ ) while  $dt \simeq n\tau_0 d_1$  near the shoreline. Such linear behaviour of  $dt$  as a function of  $d_1$  is needed to make the solution go up to  $d_1 = O(10^{-12})$  near the shoreline (for lower values of  $d_1$  the computation is stopped, as stated above). The request for  $d_1 = O(10^{-12})$  near the shoreline is due to the fact that the accuracy on the seaward side of the shock wave is generally smaller. In fact, as a consequence of the results found in §3.3, it is  $d_2 \simeq \sqrt{d_1} = O(10^{-6})$  and  $c_2 = \sqrt{d_2} = O(10^{-3})$  near the shoreline.

The total computational time is about 20 s for  $\alpha_2 = 2.3$ . In this case, the accuracy of the solution is shown in figure 3(a), where the absolute error between the theoretical value of  $\alpha_2$  and that obtained through numerical implementation are provided. The maximum error is about  $1 \times 10^{-4}$  and decreases as the shock propagates towards the shore, proving that (6.1) is a good choice for the time step. The error caused in the evaluation of shock relations is of the same order as in the machine precision,



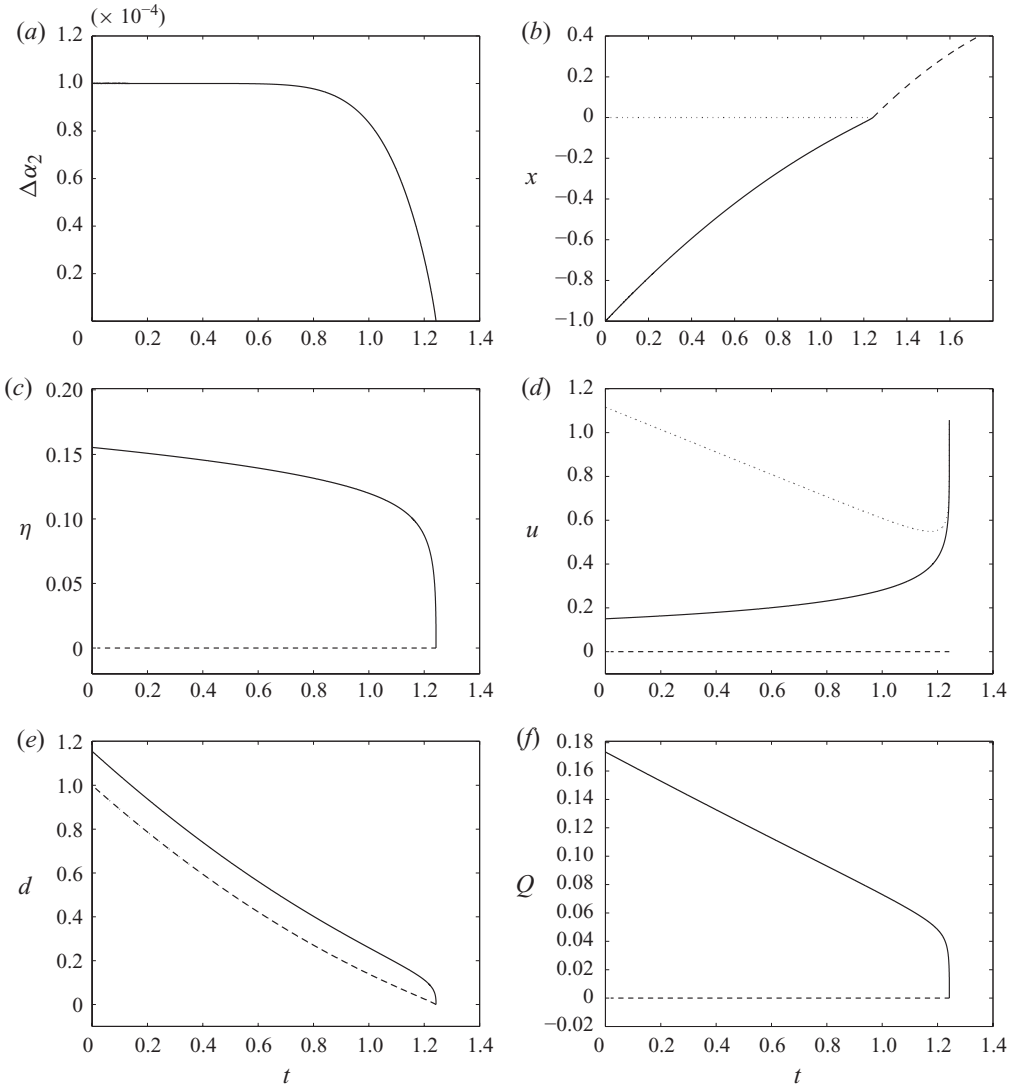


FIGURE 3. The shock solution for  $\alpha_2 = 2.3$ . (a) The absolute error ( $\Delta\alpha_2$ ) between  $\alpha_2$  and its value as computed by numerical integration of (5.2). (b) The shock path (solid line), the still shoreline (dotted line) and the shoreline after the shock arrival (dashed line). (c)–(f) The pairs  $(\eta_2, \eta_1)$ ,  $(u_2, u_1)$ ,  $(d_2, d_1)$  and  $(Q_2, Q_1)$ , respectively. The solid lines represent the quantities behind the shock while the dashed lines show the quantities in front of the shock. The dotted line in (d) represents the shock velocity  $s$ .

that is,  $2.22 \times 10^{-16}$ . Figure 3(b) shows the shock path from the seaward boundary up to the still shoreline. We define the shoreline  $x_N$  as the curve separating the wet part of beach from the dry one. Such a definition is equivalent to setting  $\dot{x}_N = u$  (the dot indicating the  $t$ -derivative). Along  $x_N$  we assume  $c = 0$ . Using the definition of  $x_N$  together with the definitions of  $\alpha$  and  $\beta$ , we can rewrite the condition as  $\dot{x}_N = \alpha - t$ . Since behind the shock  $\alpha \equiv \alpha_2$ , we get the solution

$$x_N(t) = x_0 + \alpha_2(t - t_0) - \frac{t^2}{2} + \frac{t_0^2}{2}, \quad (6.2)$$

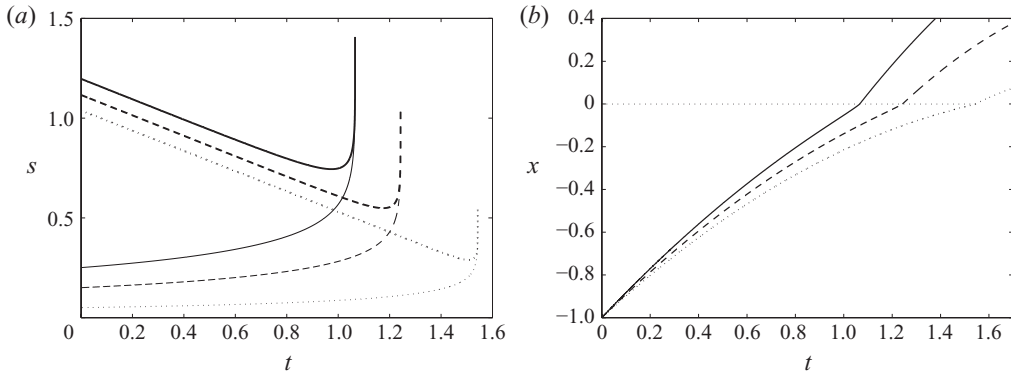


FIGURE 4. (a) The shock velocity (thick lines) and  $u_2$  (thin lines). (b) The shock path (the thin dotted line represents the still shoreline). In all panels  $\alpha_2 = 2.1$  (dotted lines), 2.3 (dashed lines) and 2.5 (solid lines).

where  $x_0$  and  $t_0$  are the  $x$ - and  $t$ -coordinates at which the shock reaches the shoreline. Note that such a solution, which is represented by a dashed line in figure 3(b), is similar to that given by Shen & Meyer (1963). Finally, in figures 3(c)–(f) the pairs  $(\eta_2, \eta_1)$ ,  $(u_2, u_1)$ ,  $(d_2, d_1)$  and  $(Q_2, Q_1)$  are shown. Moreover, in figure 3(d) the shock wave velocity has been drawn (the dotted line), showing that  $s$  converges to  $u_2$  as  $d_1$  approaches zero. Note that the bore collapse at the shoreline leads to a rapid change in the trend of all the quantities above and an increase in the size of their time derivatives, which become unbounded at the shoreline. However, as proved in Appendix A, the solution is always bounded.

In figure 4 we show the comparison between the shock velocity (a) and the shock path (b) for different values of  $\alpha_2$  (the shock path is drawn together with the shoreline evolution behind it). As expected, the dynamics are stronger as  $\alpha_2$  increases, even if the global behaviour is quite similar.

### 7. The solution behind the shock wave

Using the characteristic curves it is possible to build the flow field behind the shock wave. First, using (2.2), we rewrite the second expression of (2.3) as

$$\frac{dx}{dt} = \left( \frac{\alpha_2 + 3\beta}{4} - t \right) \quad \text{on curves such that } \beta = \text{constant}, \quad (7.1)$$

and, integrating, we obtain

$$x = x_s + \left( \frac{\alpha_2 + 3\beta}{4} \right) (t - t_s) - \frac{t^2}{2} + \frac{t_s^2}{2}, \quad (7.2)$$

where  $(t_s, x_s)$  denotes the point along the bore intersected by the specific  $\beta$ -characteristic curve. For the sake of clarity, we prefer to use the symbol  $\beta$  for the solution in the fluid region behind the shock and  $\beta_2$  for the solution along the rear side of the shock wave, even if they represent the same value. Indeed, the  $\beta$ -characteristic curve carries the values of  $\beta_2$  from the rear side of the shock wave to the fluid region behind it. In the following we just use the symbol  $\beta$ .

A straightforward representation of the shock wave provides  $t_s$  as independent variable and  $x_s = x_s(t_s)$ ,  $\beta = \beta(t_s)$ . However, as proved in Appendix B, it is possible

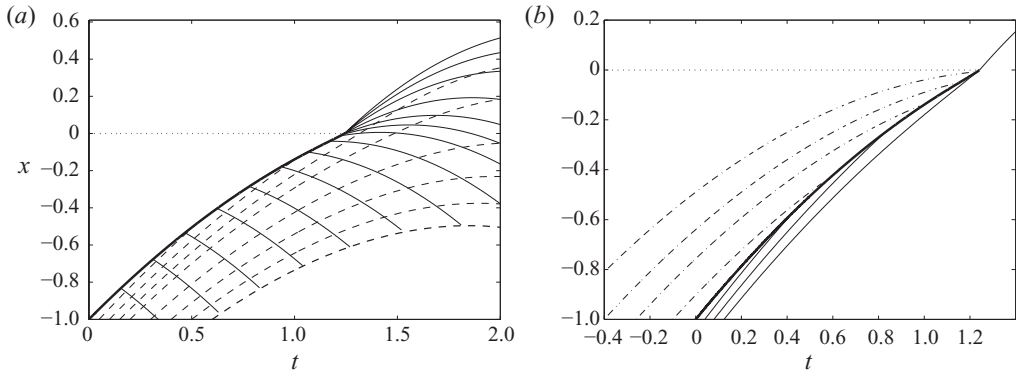


FIGURE 5. (a) The  $\beta$ -characteristic and  $\alpha$ -characteristic curves (the shock is represented by thick solid lines). (b) A sketch of the  $\alpha$ -characteristic curve collapse along the shock wave. In both panels  $\alpha \equiv 2.3$ .

and more convenient to use  $\beta$  as independent variable and write  $t_s = t_s(\beta)$  and, consequently,  $x_s = x_s(t_s(\beta)) = x_s(\beta)$ . This means that both  $t_s$  and  $x_s$  univocally depend on the chosen value of  $\beta$ . As a consequence of this choice, (7.2) depends only on  $x$ ,  $t$  and  $\beta$ . In Appendix B, we prove that for each pair  $(t, x)$  with  $t \geq t_s(\beta)$ , it is possible to make  $\beta$  explicit (that is,  $\beta = \beta(t, x)$ ) and that such a solution is unique. Since  $\alpha \equiv \alpha_2$ , it is possible to get the physical variables  $d$  and  $u$  in the region behind the shock through (2.2). The specific value of  $\beta(t, x)$  is obtained by means of numerical evaluation. The uniqueness of  $\beta(t, x)$  ensures that as long as the boundary condition described in § 4 holds, no further breaking waves are generated inside the  $\alpha$ -constant region.

Using  $\beta(t, x)$ , it is possible to integrate the first equation of (2.3) and obtain the  $\alpha$ -characteristic curves. In figure 5(a), we show the path of the  $\alpha$ - and  $\beta$ -characteristic curves, while in figure 5(b), the collapse of the former ones along the shock wave is depicted.

We recall that the validity of the present solution is subject to the condition  $\alpha \equiv \alpha_2$  which, in turn, depends on the seaward boundary assignment. From the theory of hyperbolic systems, we know that, as long as the solution is continuous, the  $\alpha$ -constant region is bounded by the last  $\alpha$ -characteristic curve which generates from the incoming signal  $u^l(t)$  at the seaward boundary. Such a curve is represented by the thick dashed line in figure 5(a). (In this figure we assigned the boundary datum  $u^l(t)$  up to  $t = 0.6$ .) In principle a shock wave can occur in the fluid domain aside the  $\alpha$ -constant region and then modify the extension of such a region. In any case, if the condition  $\alpha \equiv \alpha_2$  holds for all  $t > 0$ , we get the solution shown in figure 6 (in this case  $\alpha_2 \equiv 2.3$ ). It corresponds to a single run-up/run-down event followed by a sudden water withdrawal. Note that even though the starting jumps are not very large ( $[d] \simeq [u] \simeq 0.16$  at  $x = -1$ ), the maximum run-up given by (6.2) is quite large ( $R_{up} \simeq 0.6$ ). Incidentally, we highlight that the  $\beta$ -characteristic curves (figure 6a) coincide with the contour lines of the water depth.

In figure 7 we show the solution for the flow velocity and the water depth at a fixed  $x$ -coordinate ( $x^*$  in the figure) and for all times. Again, we denote by  $u$  and  $d$  the solutions inside the region with  $\alpha$  constant, since we prefer using the symbols  $u_2$  and  $d_2$  for the solutions along the rear side of the shock wave. In figure 7(a), we show the comparison between the flow velocity at the seaward boundary as computed through

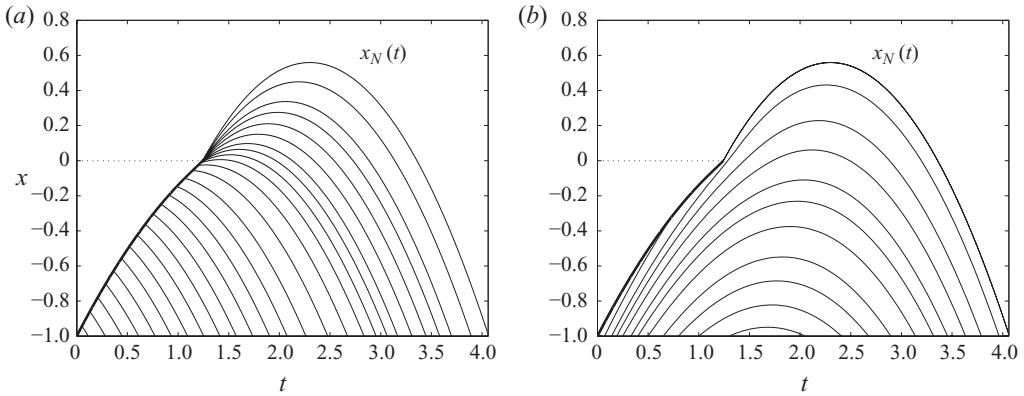


FIGURE 6. (a) The  $\beta$ -characteristic curves. (b) The  $\alpha$ -characteristic curves (the shock is represented by thick solid lines). In both panels  $\alpha \equiv 2.3$ .

numerical integration of (5.3) and the incoming signal  $u^I(t)$  given in (4.5) which was derived starting only from theoretical considerations.

The comparison is consistent up to  $t = t_{crit} = 1.6640$  when the flow at the seaward boundary becomes critical. For  $t > t_{crit}$  the flow is supercritical and, therefore, it is no longer possible to assign continuous data at the seaward boundary (even if a new shock wave is admissible since it would make the flow subcritical). In any case, the match between the two data is very good, especially during the initial stages. (The same is true for  $c^I(t)$ , which is not shown.) This is due to the fact that the reflected signals are almost zero during the first instants of the shock evolution, while they become ever larger for longer times. This also validates our previous analysis on the incoming/reflected components and on the  $\alpha$ -constant N-wave. Finally, such a result also proves that  $u^I(t)$  and  $c^I(t)$  can be effectively used as approximations of  $u(t, -1)$  and  $c(t, -1)$  during the boundary data assignment.

With regard to the water depth, figure 7(b, d, f, h) clearly shows that the swash event caused by the shock collapse is made of a thin film of water. Specifically, at  $x^* = 0.0$  and  $x^* = 0.25$  the water depth decreases from  $O(10^{-2})$  up to  $O(10^{-3})$ . This is further confirmed by figure 8, where we illustrate the total water depth at fixed times ( $t^*$  in the panels). The instant  $t^* = 1.2426$  corresponds to the time at which the shock wave reaches the shoreline, while  $t^* = \alpha_2 = 2.3$  is the instant at which the maximum run-up occurs. The shape of such a run-up/run-down solution suggests a relationship between the present model solution and that proposed by Shen & Meyer (1963). This is analysed in the following section.

Finally, figure 9 shows the flow velocity at fixed times ( $t^*$  in the panels). The velocity profile at  $t^* = 1.3426$  proves that the maximum onshore velocity is reached somewhere after the bore collapses ( $t^* = 1.2426$ ) and before the maximum run-up is reached ( $t^* = 2.3$ ). Specifically, at  $t^* = 2.3$  the velocity is negative, except at the point of maximum run-up, where it is zero.

### 7.1. Comparison with the Shen & Meyer (1963) solution

As explained in §1, the Shen & Meyer (1963) solution is an asymptotic result of the propagation of a bore into water at rest near the shoreline. The similarities with the solution shown in §7 are many. First, their solution is obtained with the assumption that  $\alpha \equiv 2$  in a neighbourhood of the shock wave and of the shoreline generating after its collapse. After the Shen & Meyer (1963) solution is adapted to the notation

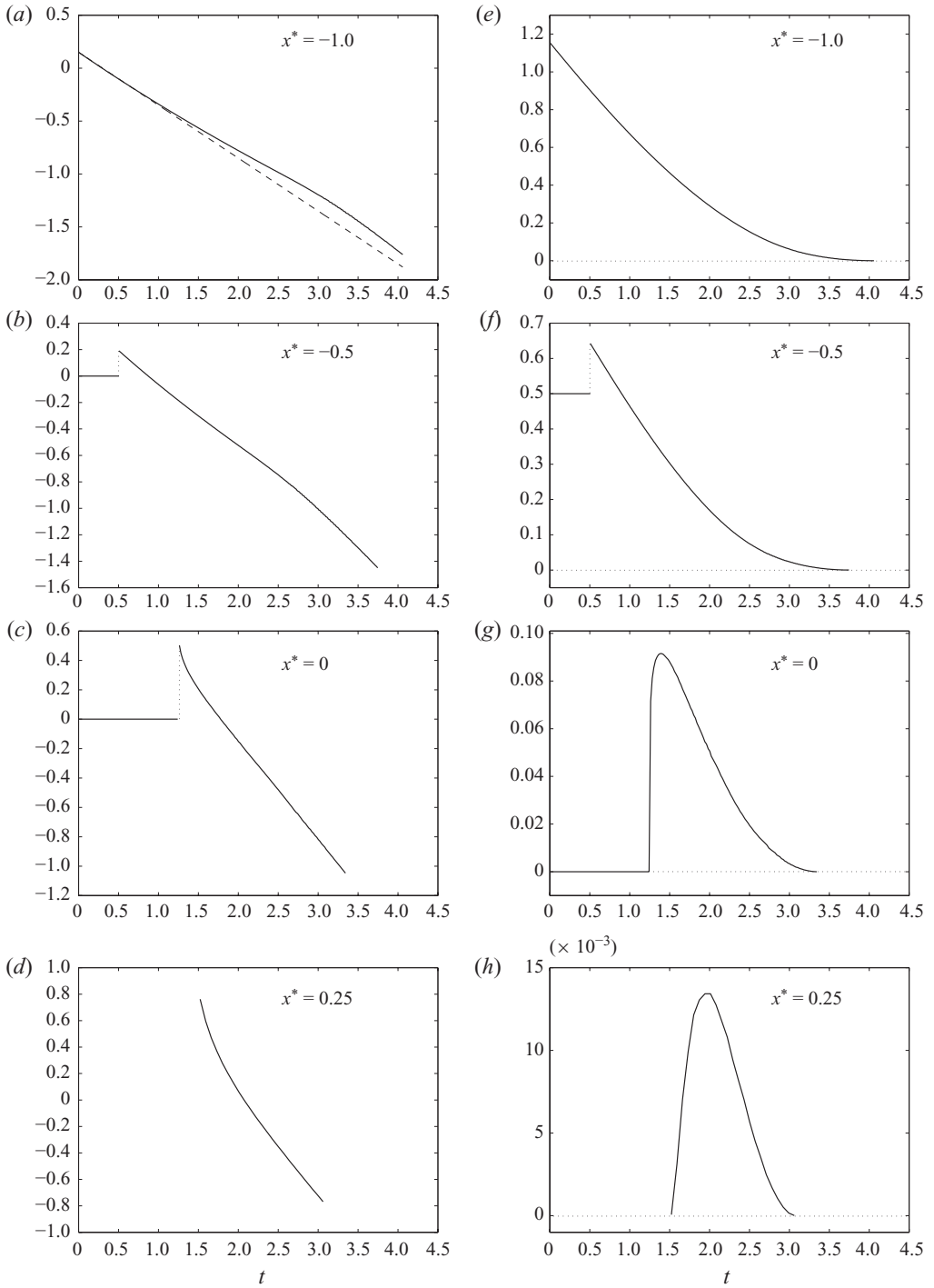


FIGURE 7. (a)–(d) The flow velocity,  $u(t, x^*)$  (the dashed line in (a) represents  $u^l$ ). (e)–(h) The total water depth,  $d(t, x^*)$ . In all panels  $\alpha_2 = 2.3$ .

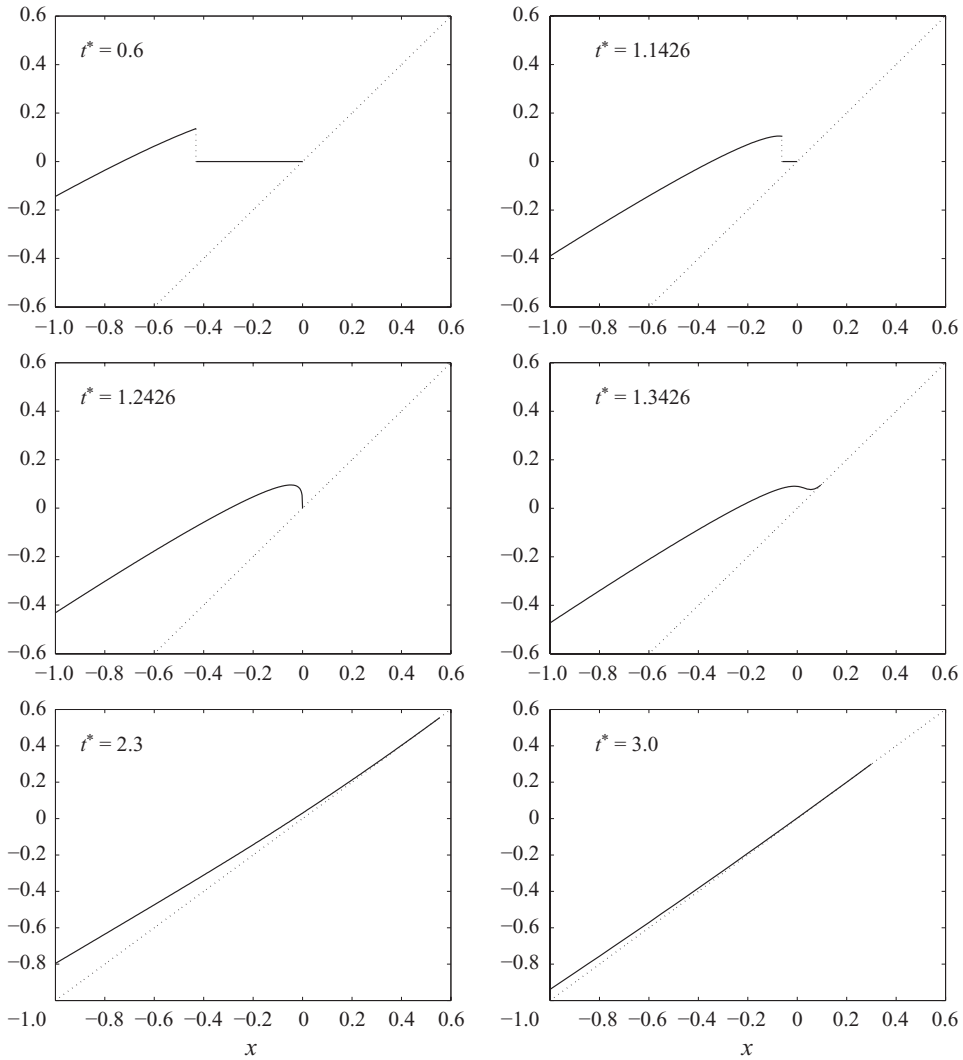


FIGURE 8. The total water depth,  $d(t^*, x)$  (solid lines). The thick dotted lines represent the beach bottom. In all panels  $\alpha_2 = 2.3$ .

used in the present study, it reads

$$d(x, t) = \frac{1}{9(t - t_0)^2} (x - x_N(t))^2, \tag{7.3}$$

where

$$x_N(t) = x_0 + 2(t - t_0) - \frac{(t - t_0)^2}{2} \tag{7.4}$$

is the shoreline, and  $x_0$  and  $t_0$  are the  $x$ - and  $t$ -coordinates at which the shock reaches the shoreline. Note that the  $x$ -derivative of the water depth at the shoreline is null, which differs from the classic solution by Carrier & Greenspan (1958) for non-breaking waves. It is simple to prove that such a property is intrinsic to every solution built on the assumption that the  $\alpha$ -field is constant. Indeed, let us consider

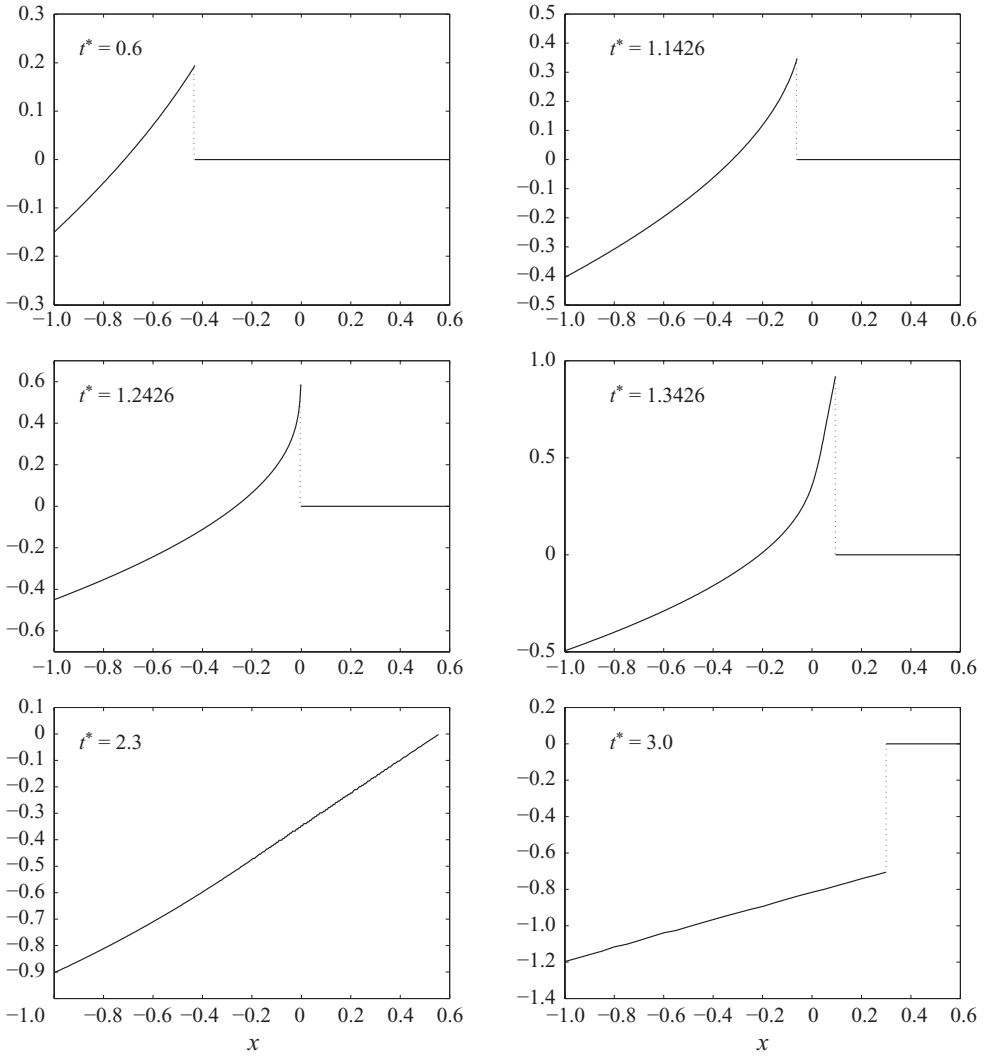


FIGURE 9. The flow velocity,  $u(t^*, x)$  (solid lines). In all panels  $\alpha_2 = 2.3$ .

the constitutive equation of the shoreline. We have

$$\frac{dx_N}{dt} = u(t, x_N(t)) = \alpha(t, x_N(t)) - t = \alpha_2 - t. \quad (7.5)$$

Then, taking the  $t$ -derivative, we get

$$\frac{d^2x_N}{dt^2} = u_t|_{x=x_N} + u|_{x=x_N} u_x|_{x=x_N} = -1. \quad (7.6)$$

By comparison with the momentum equation of the NSWEs, we immediately obtain the following:

$$d_x|_{x=x_N} = 0. \quad (7.7)$$

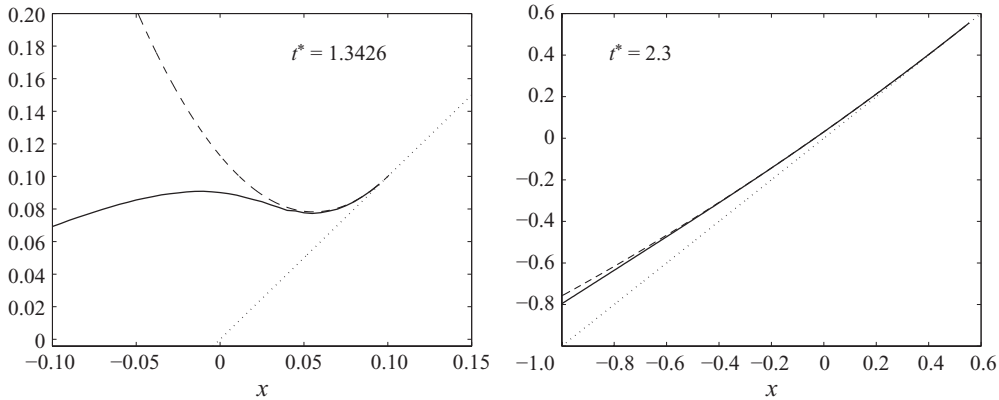


FIGURE 10. The total water depth,  $d(t^*, x)$  (solid lines) and the Shen & Meyer (1963) asymptotic solution (dashed lines). The thick dotted lines represent the beach bottom. In all panels  $\alpha_2 = 2.3$ .

Now, we come back to the present model solution and, using the result above and expanding  $d(x, t)$  in a Taylor series near the shoreline, we find

$$d(x, t) = \frac{1}{2} d_{xx}|_{x=x_N} (x - x_N(t))^2 + O((x - x_N(t))^3), \tag{7.8}$$

where  $x_N(t)$  is given by (6.2). By comparison between (7.3) and (7.8), the Shen & Meyer (1963) solution gives

$$d_{xx}|_{x=x_N} = \frac{2}{9(t - t_0)^2}, \tag{7.9}$$

where  $x_N(t)$  is now given by (7.4). In Appendix C we prove that this result does not depend on the specific value of  $\alpha_2$  and, thus, it is identical for all the solutions built on the assumption that  $\alpha$  is constant. However, since the higher contributions generally depend on  $\alpha_2$  and the flow conditions shoreward of the shock, the present model global solution represents an extension and a generalization of the Shen & Meyer (1963) asymptotic solution. Finally, in figure 10 a comparison between the two solutions is provided which confirms the identical asymptotic behaviour at the shoreline.

Since  $d_{xx} \rightarrow \infty$  as  $t \rightarrow t_0^+$ , the Shen & Meyer (1963) solution is usually said to be singular at  $t = t_0$ . However, this is just an apparent singularity. Indeed, let us denote by  $\mathcal{J}(t)$  the neighbourhood of validity of the Taylor expansion through which the formula (7.3) is obtained. As proved in § 3.3, the limit for  $t \rightarrow t_0^+$  of the water depth is zero. This implies that  $\mathcal{J}(t)$  must reduce to the point  $x_N(t_0)$  as  $t \rightarrow t_0^+$ . Further, it must reduce in such a way that a generic point  $x$  inside the neighbourhood must converge to  $x_N(t_0)$  faster than  $(t - t_0)^2$  goes to zero. In this way the water depth of (7.3) converges to zero.

## 8. Conclusions

Starting from the unique assumption of constant incoming Riemann invariant  $\alpha$ , a novel shock solution has been found for the NSWs. Such a solution differs from the results available in the literature since: (i) it describes the global evolution of the shock wave inside the sloping region and, therefore, is not restricted to narrow zones of the fluid domain; (ii) it is based not on a dam break problem but on the natural propagation of the shock wave from the seaward boundary up to the shoreline. An



in-depth analysis has been provided for the seaward boundary data assignment, and a special N-wave profile has been found such that it generates the  $\alpha$ -constant field. The result has been studied in the specific case in which the flow in front of the shock wave is still providing a large fan of solutions for the flow quantities along the shock wave and behind it. A simple theoretical inspection reveals that the Shen & Meyer (1963) solution is a particular case of the general solution proposed here. Further, the clear and simple description of the seaward boundary conditions makes the comparison with numerical simulations straightforward. For these reasons, the present shock wave solution can be regarded as a useful benchmark for the numerical solvers based on the NSWEs (see, for example, Bokhove 2005; Briganti & Dodd 2009; Kubatko *et al.* 2009).

This work was partially funded by the Italian Ministero dei Trasporti within the framework of the ‘Programma di Ricerca INSEAN 2007–2009’ and ‘Programma sulla Sicurezza INSEAN 2009’. Finally, the author would like to thank Professor M. Brocchini and the three anonymous referees for their useful comments and suggestions.

### Appendix A. Details of derivation of (5.3) and related formulations

Let us consider (3.11) and eliminate  $u_1$  and  $u_2$  using the definition of  $\alpha$ :

$$u_1 = \alpha_1 - 2\sqrt{d_1} - t, \quad u_2 = \alpha_2 - 2\sqrt{d_2} - t. \quad (\text{A } 1)$$

Then, we get

$$(\alpha_2 - \alpha_1) - 2(\sqrt{d_2} - \sqrt{d_1}) = (d_2 - d_1) \sqrt{\frac{1}{2} \left( \frac{1}{d_2} + \frac{1}{d_1} \right)}, \quad (\text{A } 2)$$

and, using  $c_2 = \sqrt{d_2}$  and  $c_1 = \sqrt{d_1}$ , we rewrite the expression above as follows:

$$(\alpha_2 - \alpha_1) - 2(c_2 - c_1) = \frac{(c_2^2 - c_1^2)}{\sqrt{2} c_1 c_2} \sqrt{c_2^2 + c_1^2}. \quad (\text{A } 3)$$

Now, squaring and rearranging, we obtain

$$c_2^6 - 9c_1^2 c_2^4 + 8c_1^2 (\alpha_2 - \alpha_1 + 2c_1) c_2^3 - c_1^2 [2(\alpha_2 - \alpha_1 + 2c_1)^2 + c_1^2] c_2^2 + c_1^6 = 0.$$

For computational reasons, it is more convenient to define  $z = c_2/\sqrt{c_1}$  and rewrite the polynomial above as follows:

$$z^6 - 9c_1 z^4 + 8\sqrt{c_1} (\alpha_2 - \alpha_1 + 2c_1) z^3 - [2(\alpha_2 - \alpha_1 + 2c_1)^2 + c_1^2] z^2 + c_1^3 = 0. \quad (\text{A } 4)$$

As a consequence of the results found in §3.3, it is  $z = O(1)$  all over the fluid domain and, therefore, (A 4) is useful to find the asymptotic behaviour of the shock wave near the shoreline (that is, for  $c_1$  going to zero). First, let us assume

$$(\alpha_2 - \alpha_1) = (\alpha_2 - \alpha_1)|_{c_1=0} + O(c_1) = (u_2 - u_1)|_{c_1=0} + O(c_1). \quad (\text{A } 5)$$

Then, expanding (A 4) in series of  $c_1$ , we find that

$$z = 2^{1/4} \sqrt{(u_2 - u_1)|_{c_1=0}} - \sqrt{2c_1} + O(c_1), \quad (\text{A } 6)$$

which corresponds to

$$c_2 = 2^{1/4} \sqrt{(u_2 - u_1)|_{c_1=0}} \sqrt{c_1} - \sqrt{2} c_1 + O(c_1^{3/2}), \tag{A 7}$$

$$d_2 = \sqrt{2} (u_2 - u_1)|_{c_1=0} c_1 - 2^{7/4} \sqrt{(u_2 - u_1)|_{c_1=0}} c_1^{3/2} + O(c_1^2). \tag{A 8}$$

Note that the first term on the right-hand side of (A 8) is in agreement with the results of § 3.3. Finally, substituting (A 7) into the second equation of (A 1), we find that

$$u_2 = \alpha_2 - t - 2^{5/4} \sqrt{(u_2 - u_1)|_{c_1=0}} \sqrt{c_1} + 2\sqrt{2} c_1 + O(c_1^{3/2}), \tag{A 9}$$

while substituting (A 8) and (A 9) into (3.10), we get

$$s = \alpha_2 - t - 2^{5/4} \sqrt{(u_2 - u_1)|_{c_1=0}} \sqrt{c_1} + \frac{5}{\sqrt{2}} c_1 + O(c_1^{3/2}). \tag{A 10}$$

### Appendix B. Uniqueness of $\beta(t, x)$

Starting from (7.2), let us consider the following expression:

$$\phi(x, t, \beta) = -x + x_s + \left( \frac{\alpha_2 + 3\beta}{4} \right) (t - t_s) - \frac{t^2}{2} + \frac{t_s^2}{2}. \tag{B 1}$$

According to Dini's theorem, the condition  $\phi_\beta \neq 0$  ensures that a unique solution  $\beta(x, t)$  of the equation  $\phi = 0$  exists. First, we compute  $\phi_\beta$  and rewrite it as follows:

$$\phi_\beta(x, t, \beta) = \dot{t}_s \left[ s - \left( \frac{\alpha_2 + 3\beta}{4} \right) + t_s \right] + (t - t_s), \tag{B 2}$$

the dot here indicating the  $\beta$ -derivative (note that  $s = \dot{x}_s/\dot{t}_s$ ). The expression above is equivalent to

$$\phi_\beta(x, t, \beta) = \dot{t}_s (s - u_2 + c_2) + (t - t_s), \tag{B 3}$$

and, since  $s \geq u_2$  (see (3.10)) and  $t \geq t_s$ , we just have to prove that  $\dot{t}_s \geq 0$ . Indeed, in this case, it would be  $\phi_\beta > 0$  and  $\phi_\beta = 0$  only at the point where the shock reaches the shoreline. This point represents a singularity since here  $\beta = \alpha_2$ , the  $\beta$ -characteristic curve coincides with the  $\alpha$ -characteristic curve and they both coincide with the shoreline. In any case, this does not present a problem for the present solution.

To prove that  $\dot{t}_s \geq 0$ , we first have to find the sign of  $\dot{s}$ . Then, we compute the  $\beta$ -derivative of (3.9). We get

$$\dot{s} = \frac{1}{2\sqrt{2}\sqrt{d_2^2/d_1 + d_2}} \left( 2 \frac{d_2}{d_1} \dot{d}_2 + \dot{d}_2 \right) \leq 0, \tag{B 4}$$

since  $\dot{d}_2 = -(\alpha_2 - \beta)/8 \leq 0$ . (Note that  $c_2 \geq 0$  implies  $\alpha_2 \geq \beta$ .) Finally, we compute the  $\beta$ -derivative of (3.10) and find

$$\dot{t}_s = \frac{1}{2} - \dot{s} + \frac{1}{2\sqrt{2}\sqrt{d_1^2/d_2 + d_1}} \left( -\frac{d_1^2}{d_2^2} \dot{d}_2 \right) \geq 0. \tag{B 5}$$

Such a result justifies the use of  $\beta$  as independent variable instead of  $t_s$ . Indeed, since  $t_s(\beta)$  is a non-decreasing function of  $\beta$ , it is possible to make  $t_s$  explicit and write  $\beta(t_s)$ .

(Note that this is again a non-decreasing function of  $t_s$ .) This proves *a posteriori* that it is possible to move from  $\beta(t_s)$  to  $t_s(\beta)$  and vice versa.

Finally, using (3.14), we get the following results at the shoreline:

$$\lim_{\beta \rightarrow \alpha_2} \dot{s} = 0, \quad \lim_{\beta \rightarrow \alpha_2} \dot{t}_s = \frac{1}{2}. \tag{B 6}$$

**Appendix C. Asymptotic behaviour near the shoreline**

In this section we prove that  $d_{xx} = 2/9(t - t_0)^2$  at the shoreline and that such a result does not depend on  $\alpha_2$ . To simplify the demonstration, we first prove that  $d_{xx} = \beta_x^2/8$ , and then we complete the proof by showing that  $\beta_x = 4/3(t - t_0)$ .

*Proof C.1.* Let us expand  $\beta$  in series near the shoreline (that is, at  $x = x_N(t)$ ):

$$\beta(x, t) = \alpha_2 + \beta_x|_{x=x_N}(x - x_N(t)) + O((x - x_N(t))^2). \tag{C 1}$$

Assuming that  $d_{xx}$  evaluated at  $x = x_N(t)$  is always different from zero and using the relation (7.8) to extract  $(x - x_N(t))$ , we rewrite (C 1) as follows:

$$\beta(x, t) = \alpha_2 - \beta_x|_{x=x_N} \sqrt{\frac{2d(x, t)}{d_{xx}|_{x=x_N}}} + O((x - x_N(t))^{3/2}), \tag{C 2}$$

where the negative sign has been chosen because  $(x - x_N(t)) \leq 0$ . Since  $d = (\alpha_2 - \beta)^2/16$ , it follows that

$$\beta(x, t) = \alpha_2 - \beta_x|_{x=x_N} \frac{(\alpha_2 - \beta(x, t))}{\sqrt{8d_{xx}|_{x=x_N}}} + O((x - x_N(t))^{3/2}), \tag{C 3}$$

and finally

$$\sqrt{8d_{xx}|_{x=x_N}} = \beta_x|_{x=x_N} + O\left(\frac{(x - x_N(t))^{3/2}}{(\alpha_2 - \beta(x, t))}\right). \tag{C 4}$$

As a consequence of (7.8),  $(x - x_N) = (\alpha_2 - \beta) + o(\alpha_2 - \beta)$  and, therefore,

$$\lim_{\beta \rightarrow \alpha_2^-} \frac{(x - x_N(t))^{3/2}}{(\alpha_2 - \beta(x, t))} = 0. \tag{C 5}$$

Then, the expansion in (C 4) is well-posed and leads to the following relation:

$$d_{xx}|_{x=x_N} = \frac{1}{8}(\beta_x|_{x=x_N})^2. \tag{C 6}$$

□

Note that, as in the Shen & Meyer (1963) solution, the result shown in Proof C.1 implies that  $d_{xx} \geq 0$  at the shoreline. This means that the depth profile near the shoreline is convex.

In the following theorem, we prove that  $\beta_x = 4/3(t - t_0)$  at  $x = x_N(t)$ . To evaluate  $\beta_x$  at the shoreline, we consider a generic  $\beta$ -characteristic curve emanating from the shock wave and the shoreline equation (6.2). Since the latter coincides with a  $\beta$ -characteristic curve with  $\beta = \alpha_2$ , this allows us to evaluate the variation of  $\beta$  in the  $x$ -direction (see, for example, the sketch in figure 11).

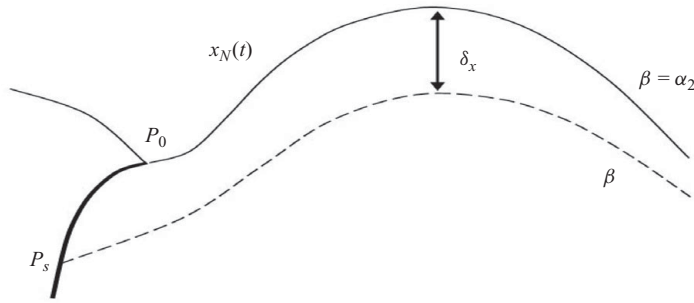


FIGURE 11. Sketch of the solution strategy for Proof C.2. The thick solid line represents the shock waves while the dashed line represents a generic  $\beta$ -characteristic curve.

*Proof C.2.* Let us consider the equation of a  $\beta$ -characteristic curve emanating from the shock wave at the point  $P_s = (t_s, x_s)$ ,

$$x = x_s + \left( \frac{\alpha_2 + 3\beta}{4} \right) (t - t_s) - \frac{t^2}{2} + \frac{t_s^2}{2}, \tag{C7}$$

and the equation of the shoreline,

$$x_N = x_0 + \alpha_2 (t - t_0) - \frac{t^2}{2} + \frac{t_0^2}{2}, \tag{C8}$$

which is generated at the point  $P_0 = (t_0, x_0)$  where the shock wave collapses. Subtracting (C8) from (C7) and rearranging, we obtain

$$x - x_N = x_s - x_0 + \frac{3}{4} (\beta - \alpha_2) (t - t_s) - \alpha_2 (t_s - t_0) + \left( \frac{t_s + t_0}{2} \right) (t_s - t_0). \tag{C9}$$

Then, using (C1), we write

$$\begin{aligned} x - x_N &= x_s - x_0 + \frac{3}{4} \beta_x|_{x=x_N} (x - x_N) (t - t_s) - \alpha_2 (t_s - t_0) \\ &\quad + \left( \frac{t_s + t_0}{2} \right) (t_s - t_0) + O((x - x_N)^2), \end{aligned}$$

and dividing by  $(t_s - t_0)$ , we finally obtain

$$\begin{aligned} \left( \frac{x - x_N}{t_s - t_0} \right) &= \left( \frac{x_s - x_0}{t_s - t_0} \right) + \frac{3}{4} \beta_x|_{x=x_N} \left( \frac{x - x_N}{t_s - t_0} \right) (t - t_s) - \alpha_2 \\ &\quad + \left( \frac{t_s + t_0}{2} \right) + O \left( \frac{(x - x_N)^2}{(t_s - t_0)} \right). \end{aligned} \tag{C10}$$

Now, let us consider the limit  $t_s \rightarrow t_0$ . In this case, the  $\beta$ -characteristic curves tend to superimpose the shoreline and, consequently,  $x \rightarrow x_N$ . Since  $x$  and  $x_N$  are both  $\beta$ -characteristic curves, we can write

$$\lim_{t_s \rightarrow t_0} \left( \frac{x - x_N}{t_s - t_0} \right) = \lim_{t_s \rightarrow t_0} \frac{x(t, \beta) - x(t, \alpha_2)}{t_s - t_0}. \tag{C11}$$

□

As shown in Appendix B, all the quantities along the seaward side of the shock wave can be expressed as functions of  $\beta$ . Then,  $t_s = t_s(\beta)$ ,  $t_0 = t_s(\beta = \alpha_2)$  and (C 11) becomes

$$\lim_{t_s \rightarrow t_0} \left( \frac{x - x_N}{t_s - t_0} \right) = \lim_{\beta \rightarrow \alpha_2} \left( \frac{x(t, \beta) - x(t, \alpha_2)}{\beta - \alpha_2} \right) \left( \frac{\beta - \alpha_2}{t_s(\beta) - t_s(\alpha_2)} \right) = 2x_\beta(t, \beta)|_{\beta=\alpha_2},$$

where the second asymptotic expression in (B 6) has been used to get the correct result. Then, assuming

$$x_\beta(t, \beta)|_{\beta=\alpha_2} \neq 0, \quad (\text{C } 12)$$

and, recalling that

$$\lim_{t_s \rightarrow t_0} \left( \frac{x_s - x_0}{t_s - t_0} \right) = s|_{x=x_N} = u_2|_{x=x_N} = \alpha_2 - t_0, \quad (\text{C } 13)$$

the expansion in (C 10) gives

$$\beta_x|_{x=x_N} = \frac{4}{3(t - t_0)}. \quad (\text{C } 14)$$

Note that such a result does not depend on  $\alpha_2$ . □

As a consequence of Proofs C.1 and C.2, we immediately find that

$$d_{x,x}|_{x=x_N} = \frac{2}{9(t - t_0)^2}. \quad (\text{C } 15)$$

These results are completely general, since they do not depend on the flow conditions shoreward of the shock wave and are only subjected to the hypothesis that  $\alpha_2$  is identically constant.

## REFERENCES

- ANTUONO, M. & BROCCINI, M. 2007 The boundary value problem for the nonlinear shallow water equations. *Stud. Appl. Math.* **119**, 73–93.
- ANTUONO, M. & BROCCINI, M. 2008 Maximum run-up, breaking conditions and dynamical forces in the swash zone: a boundary value approach. *Coast. Engng* **55** (9), 732–740.
- ANTUONO, M., HOGG, A. J. & BROCCINI, M. 2009 The early stages of a shallow flow in an inclined flume. *J. Fluid Mech.* **633**, 285–309.
- BOKHOVE, O. 2005 Flooding and drying in discontinuous Galerkin finite element discretizations of shallow-water equations. Part 1. One dimension *J. Sci. Comput.* **22–23** (1–3), 47–82.
- BRIGANTI, R. & DODD, N. 2009 Shoreline motion in nonlinear shallow water coastal models. *Coast. Engng* **56**, 495–505.
- BROCCINI, M. & DODD, N. 2008 Nonlinear shallow water equations modeling for coastal engineering. *J. Waterway Port Coast. Ocean Engng* **134**, 104–120.
- BROCCINI, M. & PEREGRINE, D. H. 1996 Integral flow properties of the swash zone and averaging. *J. Fluid Mech.* **317**, 241–273.
- CHANG, Y.-H., HWANG, K.-S. & HWUNG, H.-H. 2009 Large-scale laboratory measurements of solitary wave inundation on a 1:20 slope. *Coast. Engng.* **56** (10), 1022–1034.
- ELFRINK, B. & BALDOCK, T. E. 2002 Hydrodynamics and sediment transport in the swash zone: a review and perspectives. *Coast. Engng* **45**, 149–167.
- GUARD, P. A. & BALDOCK, T. E. 2007 The influence of seaward boundary conditions on swash zone hydrodynamics. *Coast. Engng* **54**, 321–331.
- HIBBERD, S. & PEREGRINE, D. H. 1979 Surf and run-up on a beach: a uniform bore. *J. Fluid Mech.* **95**, 323–345.
- KUBATKO, E. J., BUNYA, S., DAWSON, C., WESTERINK, J. J. & MIRABITO, C. 2009 A performance comparison of continuous and discontinuous finite element shallow water models. *J. Sci. Comput.* **40** (1–3), 315–339.

- PEREGRINE, D. H. & WILLIAMS, S. H. 2001 Swash overtopping a truncated plane beach. *J. Fluid Mech.* **440**, 391–399.
- PRITCHARD, D., GUARD, P. A. & BALDOCK, T. E. 2008 An analytical model for bore-driven run-up. *J. Fluid Mech.* **610**, 183–193.
- PRITCHARD, D. & HOGG, A. J. 2005 On the transport of suspended sediment by a swash event on a plane beach. *Coast. Engng.* **52**, 1–23.
- RYRIE, S. C. 1983 Longshore motion generated on beaches by obliquely incident bores. *J. Fluid Mech.* **129**, 193–212.
- SHEN, M. C. & MEYER, R. E. 1963 Climb of a bore on a beach. Part 3. Run-up. *J. Fluid Mech.* **16**, 113–125.
- STOKER, J. J. 1957 *Water Waves*. Interscience.
- SYNOLAKIS, C. E. 1987 The run-up of solitary waves. *J. Fluid Mech.* **185**, 523–545.
- TORO, E. F. 1999 *Riemann Solvers and Numerical Methods for Fluid Dynamics*, 2nd edn. Springer.
- TORO, E. F. 2001 *Shock Capturing Methods for Free-Surface Shallow Flows*. Wiley.
- WHITHAM, G. B. 1958 On the propagation of shock waves through regions of non-uniform area or flow. *J. Fluid Mech.* **4** (4), 337–360.
- WU, Y. & CHEUNG, K. F. 2007 Explicit solution to the exact Riemann problem and application in nonlinear shallow-water equations. *Intl J. Numer. Methods Fluids* **57** (11), 1649–1668.
- ZHANG, Q. & LIU, P. L.-F. 2008 A numerical study of swash flows generated by bores. *Coast. Engng* **55**, 1113–1134.